



Technical note: Use of PM_{2.5} to CO ratio as a tracer of wildfire smoke in urban areas

Daniel A. Jaffe^{1,2}, Brendan Schnieder³ and Daniel Inouye³

5 ¹School of STEM, University of Washington, Bothell, WA, 98011, USA

²Department of Atmospheric Sciences, University of Washington, Seattle, WA, 98195, USA

³Washoe County Health District, Air Quality Management Division, Reno, NV, USA

Correspondence to: Daniel A. Jaffe (djaffe@uw.edu)

Abstract. Wildfires, and the resulting smoke, are an increasing problem in many regions of the world. However, identifying
10 the contribution of smoke to pollutant loadings in urban regions can be challenging at lower concentrations due to the presence
of the usual array of anthropogenic pollutants. Here we propose a method using the difference in PM to CO emission ratios
between smoke and typical urban pollution. For smoke, emission ratios of PM_{2.5} to CO are between 200-300 µg m⁻³ ppb⁻¹,
whereas typical urban sources have an emission ratio that is lower by a factor of 4-10. This gives rise to the possibility of
using this ratio as an indicator of smoke extent. We use observations at a regulatory surface monitoring site in Sparks, NV, for
15 the period of May-September 2018-2021. During this time, there were many smoke-influenced periods from numerous
California wildfires that burned during this period. Using a PM/CO ratio of 30, we can split the data into smoke-influenced
and no-smoke periods. We then develop a Monte Carlo simulation, tuned to local conditions, to derive a set of PM_{2.5} /CO
values that can be used to identify smoke influence in urban areas. From the simulation, we find that a smoke enhancement
ratio of 140 µg m⁻³ ppb⁻¹ best fits the observations, which is significantly lower than the ratio observed in fresh smoke plumes.
20 The most likely explanation for this difference is greater loss of PM_{2.5} during dilution and transport to warmer surface layers.
We find that the PM_{2.5}/CO ratio in urban areas is an excellent indicator of smoke and should prove to be useful to identify
biomass burning influence on the policy relevant concentrations of both PM_{2.5} and O₃. Using the results of our Monte Carlo
simulation, this ratio can also quantify the influence of smoke on urban PM_{2.5}.

1. Introduction

25 In the U.S., smoke has become an increasingly challenging problem due to a significant increase in the area burned by wildfires
(Zhuang et al 2021; Kalashnikov et al 2022; McClure and Jaffe 2018). Data from the National Interagency Fire Center
(www.nifc.gov) show that between the early 1980s and 2021, the decadal average annual area burned by wildfires in the U.S.
has increased by almost a factor of 3, from 1.1 to 3.0 million ha per year. Multiple factors are responsible for this increase,
including climate change, increasing human ignitions and past forest management (Jaffe et al 2020).

30 Primary emissions from fires include fine particulate matter with a diameter of less than 2.5 µm (PM_{2.5}), carbon monoxide
(CO), nitrogen oxides (NO_x=NO+NO₂), and hundreds of volatile organic compounds (VOCs), including many toxic and



hazardous air pollutants (Akagi et al 2011; Permar et al 2021). In addition, secondary chemistry leads to O₃ and other secondary products. The cumulative impact of these emissions has substantial health implications (e.g., Ebi et al 2021; O'Dell et al 2020; 2021; Gan et al 2020; Doubleday 2020; Sorenson et al 2021). Smoke at the surface can be transported from nearby or distant fires (e.g. DeBell et al 2004; Jaffe et al 2004; Teakles et al 2017; Rogers et al 2020). Satellites can provide an exceptional geospatial view of fires and the occurrence and transport of smoke (e.g. Duncan et al 2014; Jaffe et al 2020; Kahn 2020; O'Neil et al 2021; Holloway et al 2021). But with very few exceptions, satellite data provide little to no vertical information directly. Modeling of smoke transport and exposure is challenging for a number of reasons, including uncertainties in emissions, plume injection heights and model resolution (Lu 2016; O'Neill 2021; Ye 2021). It is possible to measure unique smoke markers, such as acetonitrile (CH₃CN) (Singh et al 2012; Chandra et al 2020), but these measurements are not routinely performed at surface sites, and even common tracer like acetonitrile also have some anthropogenic sources (Huangfu et al 2022).

Wildfire emissions are chemically distinct from anthropogenic, industrial or vehicular emissions in having very high PM_{2.5} emissions per unit of fuel burned. For the U.S. as a whole, the U.S. EPA reports a PM_{2.5} to CO emission ratio (ER) of 0.085 in 2017 (g/g) for all emission sources, excluding wildfires (U.S. EPA 2022). This ratio drops to 0.076 if residential wood combustion is also excluded. Akagi et al (2011) report an emission ratio of 0.12-0.14 (g/g) for temperate and extra-tropical wildfires. In urban areas, it is likely that this ratio is even lower, due to a greater contribution from mobile sources (cars and trucks), which have a PM_{2.5} to CO emission ratio of 0.009 (g/g). Observations of PM_{2.5} and CO in urban areas often show good correlation and these can be used to derive the normalized enhancement ratio (NER, $\Delta\text{PM}_{2.5}/\Delta\text{CO}$), which reflects the emissions, chemical and physical processing, and any background contribution. Reported $\Delta\text{PM}_{2.5}/\Delta\text{CO}$ NERs in urban areas from several studies are in the range of 21-45 $\mu\text{g m}^{-3} \text{ppm}^{-1}$, which would correspond to an emission ratio of 0.018-0.039 g/g, assuming no loss of either species (Dimitriou and Kassomenos, 2014; Patton et al., 2014). Laing et al (2017) looked at the PM_{2.5} to CO correlation in 8 western U.S. cities for non-smoke periods and found reasonable correlations (R^2 values of 0.32-0.57) and slopes of 21-66 with a median value of 35 $\mu\text{g m}^{-3} \text{ppm}^{-1}$ (corresponding to emission ratios of 0.018-0.057 g/g). Laing et al (2017) also found that smoke-influenced periods had much higher PM_{2.5} to CO correlation slopes ranging from 57-228, with a median of 128 $\mu\text{g m}^{-3} \text{ppm}^{-1}$ (n=25). Garofolo (2019) reported values of 80-400 $\mu\text{g m}^{-3} \text{ppm}^{-1}$, with most between 200-300 for the organic aerosol to CO NER for 20 fires during the 2018 WECAN experiment. Briggs et al (2016) report mean aerosol scattering to CO NERs of 0.90 for 23 plumes at MBO, corresponding to a PM/CO ratio of 200-300 $\mu\text{g m}^{-3} \text{ppm}^{-1}$, depending on the mass scattering efficiency and Kleinmann et al (2020) report mean values of 317 and 361 $\mu\text{g m}^{-3} \text{ppm}^{-1}$ for aged and fresh plumes, respectively, during the 2013 BBOP experiment. Selimovic et al (2019; 2020) note that the PM/CO NER in ground-level smoke is about half of that observed from aircraft or free tropospheric observations. This is most likely caused by evaporation of organic aerosol mass due to higher surface temperatures and greater downstream dilution. These past observations present a fairly consistent picture showing that PM_{2.5}/CO NER for surface smoke is about 3-4 times greater than the NER for typical urban observations in the absence of smoke, based on the medians in Laing et al 2017.



65 The very different PM_{2.5} to CO NERs for typical urban air and smoke events suggest that the observed ratios can be used to
derive the smoke contribution to surface PM_{2.5} concentrations. To examine this hypothesis, we use data from a monitoring
site in Sparks, NV, near Reno, a region that has been heavily influenced by smoke in the past several years due to the large
number and extent of California wildfires. Data from this region were recently used to examine the role of high PM_{2.5} exposure
from smoke on COVID-19 incidence (Kiser et al 2021). From the Sparks, NV observations, we develop a quantitative model
70 using a Monte Carlo simulation that provides a range of probabilistic results that can be compared to observations. We find
that this method appears to reasonably quantify the smoke contribution in an urban area.

2. Methods and data sources

For this analysis, we use daily mean PM_{2.5} and CO concentrations for May–September 2018–2021 from the Sparks, NV routine
air quality monitoring site (EPA AQS identification #320311005) near Reno, NV that is operated by the Washoe (NV) County
75 Health District, Air Quality Management Division. The site uses instruments and standards that are consistent with the national
EPA requirements (40 CFR Part 58) and report data into the EPA's national Air Quality System (AQS). The Sparks site has
near-continuous measurements of PM_{2.5}, CO and O₃. We use data for May–September 2018–2021 to avoid complications
with sources from residential wood combustion. Data were obtained from the EPA AirData site ([https://www.epa.gov/outdoor-
air-quality-data](https://www.epa.gov/outdoor-air-quality-data)), except for 2021 data, which were obtained from AirNow-Tech, a web-based data resource operated for the
80 U.S. EPA (<https://www.airnowtech.org/>). We note that 2021 data is considered preliminary at this time, although in practice
the preliminary data usually do not change significantly. Instrumentation at the Sparks site include a MetOne model 1020 Beta
Attenuation Monitor (BAM) for PM_{2.5}, a Teledyne API model 300 EU non-dispersive IR monitor for CO and a Teledyne API
model T400 UV O₃ analyser. These instruments have stated detection limits (DLs) of 1 µg m⁻³, 20 ppb and 0.4 ppb,
respectively. Because there were some zero and very low values for PM_{2.5} any concentration less than the DL was set to 1 µg
85 m⁻³. This impacted less than 2% of the dataset. No below DL values were reported for the CO or O₃ data. As an indication
of overhead smoke, we use the daily product from the NOAA Hazard Mapping System–Fire and Smoke Product (hereafter
simply HMS). This product is based on analysis of multiple satellite products, both geostationary and polar orbiting. More
details on HMS are in Rolph et al (2009) and Kaulfus et al (2017). We note that HMS can sometimes miss thin smoke
plumes, especially in the presence of clouds (Buysse et al 2019). Buysse et al (2019) found that there is enhanced surface
90 PM_{2.5} on 30–70% of the days with overhead HMS smoke, depending on the location.

3. Results

Figure 1 shows one example of the HMS smoke product for the Loyalton fire on Aug. 16, 2020, which was about 35–45 km
from the Sparks monitoring site. This fire started on 8/14/2020 and burned for approximately one month. In total, this fire
95 burned approximately 20,000 ha in the Tahoe and Humboldt-Toiyabe National Forests. On 8/16/2020, the daily mean PM_{2.5}



and CO concentrations were $38 \mu\text{g m}^{-3}$ and 0.43 ppm at the Sparks, NV monitoring site. As Washoe County is located just east of the California-Nevada border, smoke from many fires in California is often transported to the Sparks monitor. Table 1 shows data for the number of days that exceeded the U.S. National Ambient Air Quality Standards (NAAQS) for $\text{PM}_{2.5}$ (2006, 24-hour standard, daily mean of $35 \mu\text{g m}^{-3}$) and O_3 (2015 8-hour O_3 standard, maximum daily 8-hour mean of 0.070 ppm) for the Sparks monitoring site, along with the annual area burned in California. While 2020 was the highest year on record for the area burned in CA for the past 2 decades, 2021 was the second highest year and had a greater number of days in Reno that exceeded the NAAQS. Note that 2019 was a particularly low fire year in CA and there were no exceedances of either the daily $\text{PM}_{2.5}$ or O_3 NAAQS at the Sparks monitoring site. Overall, for this time period (May-September 2018-2021), 200 out of 612 days had overhead HMS smoke at the Sparks monitoring location. The $\text{PM}_{2.5}/\text{CO}$ smoke criteria is discussed later in this section.

| | 2018 | 2019 | 2020 | 2021 |
|---|-------|-------|-------|-------|
| California area burned (Ha) | 7.4E5 | 1.0E5 | 1.7E6 | 1.1E6 |
| Sparks Overhead HMS smoke (days) | 51 | 11 | 52 | 86 |
| Sparks smoke days* | 30 | 5 | 64 | 57 |
| $\text{PM}_{2.5}$ exceedance days | 6 | 0 | 19 | 22 |
| $\text{PM}_{2.5}$ exceedance days with smoke* | 6 | 0 | 19 | 22 |
| O_3 exceedance days | 10 | 0 | 5 | 13 |
| O_3 exceedance days with smoke* | 10 | 0 | 5 | 11 |

Table 1: California area burned, overhead HMS smoke days, and days over the U.S. National Ambient Air Quality Standard at Sparks, NV for $\text{PM}_{2.5}$ (daily mean of $35 \mu\text{g m}^{-3}$) and O_3 (70 ppb, 8 hour average). The smoke criteria (indicated by *) uses a $\text{PM}_{2.5}/\text{CO}$ ratios of 35, as discussed later in text.

Figure 2 shows the daily $\text{PM}_{2.5}$ vs CO concentrations for May-Sept 2018-2021, segregated for smoke vs non-smoke conditions. The data are segregated using (i) the HMS smoke product and (2) a $\text{PM}_{2.5}/\text{CO}$ ratio greater or less than 30. The value of 30 is chosen based, in part, on the work of Laing et al (2017) and on evaluation of likely smoke influence. We find the slopes and correlations are not strongly influenced by the choice of $\text{PM}_{2.5}/\text{CO}$ ratio. For example, using a ratio of <20, 30, 40 and 50 we get slopes of 16.5, 18.1, 23.4 and $33.9 \mu\text{g m}^{-3}$ per ppm, an increasing pattern as would be expected. We found that smoke influence can be observed on some days at a PM/CO ratio as low as 32. An example of this is 8/5/2018, when extensive and heavy smoke blankets most of California, Nevada and other western states. $\text{PM}_{2.5}$ and CO concentrations at Sparks are $22 \mu\text{g m}^{-3}$ and 0.68 ppm, respectively, for a $\text{PM}_{2.5}/\text{CO}$ ratio of 32. So, while the relatively low ratio implies significant mixing of this smoke event with air containing a lower ratio, the high $\text{PM}_{2.5}$ concentrations and widespread smoke is consistent with a significant smoke influence on that day. Using the $\text{PM}_{2.5}/\text{CO}$ ratio to segregate the data, we find an improved correlation of PM and CO in the lower range of ratios, compared with using the HMS alone as an indicator (Figure 2). Table 2 summarizes the dataset, as segregated by the PM/CO ratio as well as using the HMS smoke product alone. While there is relatively little change in the mean and SD of the smoke-influenced and non-smoke data, the improved correlation suggests that the $\text{PM}_{2.5}/\text{CO}$



ratio is a better way to segregate the dataset. We note that the exact choice of PM_{2.5}/CO ratio depends on the certainty required. This is discussed in more detail using a Monte Carlo simulation, as described below. We note that there are 53 days with
125 overhead HMS smoke, but a PM_{2.5}/CO ratio < 30 and 60 days with a PM_{2.5}/CO ratio > 30 and no HMS smoke.

Table 2. Sparks daily PM_{2.5} and CO data for May-September 2018-2021, segregated by the PM_{2.5}/CO ratio and by overhead HMS smoke.

| | PM _{2.5} /CO <30.0 (no smoke) | PM _{2.5} /CO >30.0 (smoke-influenced) |
|--|---|---|
| Count | 414 | 198 |
| Mean PM_{2.5} (μg m⁻³) | 4.8 | 27.7 |
| Std. Dev. (μg m⁻³) | 1.8 | 29.2 |
| | HMS=0 (no smoke) | HMS=1 (smoke-influenced) |
| Count | 412 | 200 |
| Mean PM_{2.5} (μg m⁻³) | 5.1 | 26.9 |
| Std. Dev. (μg m⁻³) | 1.9 | 29.6 |

We use the PM_{2.5} and CO data to develop a Monte Carlo simulation of the PM/CO ratio for Reno using the following
135 relationships:

$$\text{PM}_{2.5} (\mu\text{g m}^{-3}) = \text{Urban PM}_{2.5} + \text{Smoke PM}_{2.5} + \text{background PM}_{2.5} = 10^{\alpha} + 10^{\beta} + 2 \mu\text{g/m}^3 \quad (1)$$

$$\text{CO (ppm)} = \text{Urban PM}_{2.5}/R_{\text{urban}} + \text{Smoke PM}_{2.5}/R_{\text{smoke}} + 0.2 \text{ ppm} \quad (2)$$

Where R_{urban} and R_{smoke} are the NERs ($\Delta\text{PM}_{2.5}/\Delta\text{CO}$) to represent urban emissions and smoke, respectively. The smoke terms in equations 1 and 2 are only included on 1/3 of the days, corresponding to the fractional incidence of HMS smoke.
140 We explore a range of values for R_{urban} and R_{smoke} as shown in Table 3. The parameters α and β are used to model the log-normal distributions for urban PM_{2.5} with, and without, smoke PM_{2.5}, respectively. Equations 1 and 2 include a background contribution to represent natural, biogenic, and intercontinental sources of PM_{2.5} and CO. The background concentrations were set to 2 μg m⁻³ for PM_{2.5} and 0.2 ppm for CO. These background values were estimated based on observations from
145 (Cheeka Peak, WA, AQS #530090013). For the May-Sept 2019 period the West Yellowstone mean values for PM_{2.5} and CO were 2.5 μg m⁻³ and 0.24 ppm, whereas for the Cheeka Peak site the mean values were 2.1 μg m⁻³ and .08 ppm. Median values were very similar at both sites. While PM_{2.5} concentrations were similar at both sites, whereas CO was higher at the continental site. Given that Sparks, NV is a continental/inland location, the West Yellowstone, MT concentrations are likely more representative of its background concentrations.

150 The Monte Carlo simulations estimate the observed PM_{2.5} and CO concentrations, and the ratio, using Equations 1 and 2. The simulation computes 10,000 concentrations, where α , β , R_{urban} and R_{smoke} are allowed to vary independently with values as defined in Table 3. These values are chosen to be consistent with the mean and S.D. of the non-smoke (α) and smoke (β)



155 datasets, respectively, excluding the contribution from background concentrations. Note that the Monte Carlo simulations are intended to reflect the bulk distributions, so there is no correspondence between an individual day in the simulation with any particular day in the observations.

Table 3. Parameter values used in the Monte Carlo simulations. For the R_{urban} and R_{smoke} parameters, multiple mean values are considered.

| | α (unitless) | β (unitless) | R_{urban} ($\mu\text{g m}^{-3} \text{ppm}^{-1}$) | R_{smoke} ($\mu\text{g m}^{-3} \text{ppm}^{-1}$) |
|------------------|------------------------|-----------------------|--|--|
| Mean | 0.4 | 1.3 | 20,40,80 | 100,140,200 |
| Std. Dev. | 0.2 | 0.4 | 10 | 20 160 |

165 Figure 3 shows results of the simulation and with varying mean values for the R_{smoke} parameter. Even at very high $\text{PM}_{2.5}$ concentrations, the observed $\text{PM}_{2.5}/\text{CO}$ ratio never exceeded $125 \mu\text{g m}^{-3} \text{ppm}^{-1}$. The simulation suggests an optimum R_{smoke} value of $140 \mu\text{g m}^{-3} \text{ppm}^{-1}$. So, consistent with the work of Laing et al (2017) and Selimovic et al (2019; 2020), we find that the best-fit NER values at the surface are much lower than emission factors reported for fresh or free tropospheric smoke plumes.

170 Figure 4 shows the results of the simulations with varying values for the R_{urban} parameter. Here, the best value is more difficult to discern. At high $\text{PM}_{2.5}$ concentrations and PM/CO ratios, this parameter has very little influence on the simulated values. At the low range of $\text{PM}_{2.5}$ concentrations a value of 20 is clearly too low, but there is little difference between the other values and so it is not clear which value is optimal. This parameter should reflect the primary $\text{PM}_{2.5}$ and CO emissions in the area, plus contributions from secondary organic aerosol (e.g. Nault et al 2021). For Washoe County, NV (the county containing Reno and Sparks) the EPA's 2017 National Emission Inventory gives primary emissions of $\text{PM}_{2.5}$ and CO of 1,482 and 55,529 short tons per year, excluding wildfires and residential wood combustion. This corresponds to a $\text{PM}_{2.5}/\text{CO}$ emission ratio of 0.034 g/g or an enhancement ratio of $39 \mu\text{g m}^{-3} \text{ppm}^{-1}$. An important constraint on using this approach to discern the urban, non-smoke $\text{PM}_{2.5}/\text{CO}$ NER are limitations on the instrumentation and the impact of background concentrations at low $\text{PM}_{2.5}$ and CO concentrations. Nonetheless, we find that using an R_{urban} parameter of either 40 or 80 has little influence on our results at higher $\text{PM}_{2.5}$ concentrations. For the remaining of this analysis, we use an R_{smoke} value of 140 and an R_{urban} value of 40.

180 Figure 5 shows the fractional smoke contribution to $\text{PM}_{2.5}$ vs the $\text{PM}_{2.5}/\text{CO}$ NER from the Monte Carlo simulations. As specified in the model setup, 2/3 of the points have no smoke contribution. These have a mean $\text{PM}_{2.5}/\text{CO}$ value of 17, with a range of 6-34. As the Monte Carlo simulations represent a probabilistic approach, we can also look at the likelihood that a given set of points has a specific degree of smoke influence. Figure 5 shows the probability that a given set of $\text{PM}_{2.5}/\text{CO}$ ratios (binned in units of 10) has more than 50% of the $\text{PM}_{2.5}$ due to smoke. So, starting with the $\text{PM}_{2.5}/\text{CO}$ bin of 30-40, we have a very high probability (0.82) of more than 50% $\text{PM}_{2.5}$ due to smoke and at a bin of 40-50, we have near certainty (0.996).



We can use the information in Figure 5 to evaluate the likelihood that smoke contributed to the days with high PM_{2.5} or O₃, as shown in table 1. The years 2018, 2020 and 2021 all had significant number of exceedances days (over the NAAQS), whereas the low fire year of 2019 had none. For Table 1, we use a PM_{2.5}/CO values of 35 which, based on the Monte Carlo simulation, implies that smoke contributes more than half of the total PM_{2.5} on 85% of days. Even using a smoke criteria of PM_{2.5}/CO of 45, we find no change in the number of smoke influenced days. Not surprisingly, the PM_{2.5}/CO criteria identified all of the PM_{2.5} exceedance days as smoke influenced, using either smoke criteria (35 or 45). For O₃, the results show that 24 out of the 26 exceedance days were smoke influenced, using either criteria. While the PM_{2.5}/CO ratio can quantitatively estimate the fraction of PM due to smoke (e.g. Figure 5), we note that this approach can not provide a quantitative estimate of the smoke contribution to the O₃ levels. Other tools would be needed to quantify the smoke contribution to the MDA8 O₃ values (e.g. Ninneman and Jaffe 2021; Jaffe 2021; Gong et 2017). Nonetheless, the results shown in Table 1 clearly show that the PM_{2.5}/CO can identify days with a strong smoke signature.

4. Summary

The large difference in emission ratios between typical urban pollution and wildfire smoke gives rise to very different observed NERs in urban areas for non-smoke and smoke-influenced conditions. We find that a Monte Carlo simulation of mixing between smoke and non-smoke NERs can accurately reproduce the observed NERs and provides a measure of smoke influence in an urban area. The model supports earlier work that finds the PM_{2.5}/CO NER in biomass burning influenced plumes at surface sites is approximately half of that observed in fresh emissions and in cooler environments. This likely is caused by loss of PM mass during transport due to dilution and warmer temperatures at surface sites. For the Sparks, NV monitoring site we find that at a PM_{2.5}/CO ratio of 35 $\mu\text{g m}^{-3} \text{ppm}^{-1}$ biomass burning contributes more than half of the total PM_{2.5} on 85% of days. These calculations are based on the observed concentrations at one regulatory monitor, but should be applicable to other sites. To apply the Monte Carlo simulation at other sites requires that the parameters in Table 3 be adjusted to fit the local data. The R_{urban} parameter would need to be adjusted based on local emissions and observations and the α and β parameters would need to be fit based on the observed non-smoke and smoke concentrations, respectively.

This analysis demonstrates that it is possible to identify smoke at the surface based on commonly measured air pollutants with high confidence. While satellite data can also identify smoke influence, these have a high false positive rate, meaning that many days identified by satellite products as having overhead smoke show little or no influence at the surface. We propose that the observed PM_{2.5}/CO ratio provides a more robust signal of surface smoke in urban areas and with no false positives.

Acknowledgements

This work was supported by the National Oceanic and Atmospheric Administration (NOAA; grant number NA17OAR431001). The authors acknowledge helpful comments from Nathan May and Matthew Ninneman.



References

- 215 Akagi, S. K., Yokelson, R. J., Wiedinmyer, C., Alvarado, M. J., Reid, J. S., Karl, T., Crounse, J. D., and Wennberg, P. O.: Emission factors for open and domestic biomass burning for use in atmospheric models, *Atmos. Chem. Phys.*, 11, 4039-4072, <https://doi.org/10.5194/acp-11-4039-2011>, 2011.
- Brey, S. J., Ruminski, M., Atwood, S. A., and Fischer, E. V.: Connecting smoke plumes to sources using Hazard Mapping System (HMS) smoke and fire location data over North America, *Atmos. Chem. Phys.*, 18, 1745-1761, <https://doi.org/10.5194/acp-18-1745-2018>, 2018.
- 220 Buysse, C. E., Kaulfus, A., Nair, U., and Jaffe, D. A.: Relationships between particulate matter, ozone, and nitrogen oxides during urban smoke events in the western US, *Environ. Sci. Technol.*, 53, 12519-12528, <https://doi.org/10.1021/acs.est.9b05241>, 2019.
- Chandra, B. P., McClure, C. D., Mulligan, J., and Jaffe, D. A.: Optimization of a method for the detection of biomass-burning relevant VOCs in urban areas using thermal desorption gas chromatography mass spectrometry, *Atmosphere*, 11, 276, <https://doi.org/10.3390/atmos11030276>, 2020.
- 225 DeBell, L. J., Talbot, R. W., Dibb, J. E., Munger, J. W., Fischer, E. V., and Frohking, S. E.: A major regional air pollution event in the northeastern United States caused by extensive forest fires in Quebec, Canada, *J. Geophys. Res.-Atmos.*, 109, <https://doi.org/10.1029/2004jd004840>, 2004.
- 230 Doubleday, A., Schulte, J., Sheppard, L., Kadlec, M., Dhammapala, R., Fox, J., and Busch Isaksen, T.: Mortality associated with wildfire smoke exposure in Washington State, 2006–2017: a case-crossover study, *Environ. Health*, 19, 4, <https://doi.org/10.1186/s12940-020-0559-2>, 2020.
- Duncan, B. N., Prados, A. I., Lamsal, L. N., Liu, Y., Streets, D. G., Gupta, P., Hilsenrath, E., Kahn, R. A., Nielsen, J. E., Beyersdorf, A. J., Burton, S. P., Fiore, A. M., Fishman, J., Henze, D. K., Hostetler, C. A., Krotkov, N. A., Lee, P., Lin, M., Pawson, S., Pfister, G., Pickering, K. E., Pierce, R. B., Yoshida, Y., and Ziemba, L. D.: Satellite data of atmospheric pollution for U.S. air quality applications: Examples of applications, summary of data end-user resources, answers to FAQs, and common mistakes to avoid, *Atmos. Environ.*, 94, 647-662, <https://doi.org/10.1016/j.atmosenv.2014.05.061>, 2014.
- 235 Ebi, K. L., Vanos, J., Baldwin, J. W., Bell, J. E., Hondula, D. M., Errett, N. A., Hayes, K., Reid, C. E., Saha, S., Spector, J., and Berry, P.: Extreme weather and climate change: Population health and health system implications, *Annu. Rev. Publ. Health*, 42, 293-315, <https://doi.org/10.1146/annurev-publhealth-012420-105026>, 2021.
- 240 Gan, R. W., Liu, J., Ford, B., O'Dell, K., Vaidyanathan, A., Wilson, A., Volckens, J., Pfister, G., Fischer, E. V., Pierce, J. R., and Magzamen, S.: The association between wildfire smoke exposure and asthma-specific medical care utilization in Oregon during the 2013 wildfire season, *J. Expo. Sci. Environ. Epidemiol.*, 30, 618-628, <https://doi.org/10.1038/s41370-020-0210-x>, 2020.
- 245 Garofalo, L. A., Pothier, M. A., Levin, E. J. T., Campos, T., Kreidenweis, S. M., and Farmer, D. K.: Emission and evolution of submicron organic aerosol in smoke from wildfires in the western United States, *ACS Earth Space Chem.*, 3, 1237-1247, <https://doi.org/10.1021/acsearthspacechem.9b00125>, 2019.
- 250 Hadley, O., Cutler, A., Schumaker, R., and Bond, R.: Wildfires and wood stoves: Woodsmoke toxicity and chemical characterization study in the north-western United States, *Atmos. Environ.*, 253, 118347, <https://doi.org/10.1016/j.atmosenv.2021.118347>, 2021.
- Holloway, T., Miller, D., Anenberg, S., Diao, M., Duncan, B., Fiore, A. M., Henze, D. K., Hess, J., Kinney, P. L., Liu, Y., Neu, J. L., O'Neill, S. M., Odman, M. T., Pierce, R. B., Russell, A. G., Tong, D., West, J. J., and Zondlo, M. A.:



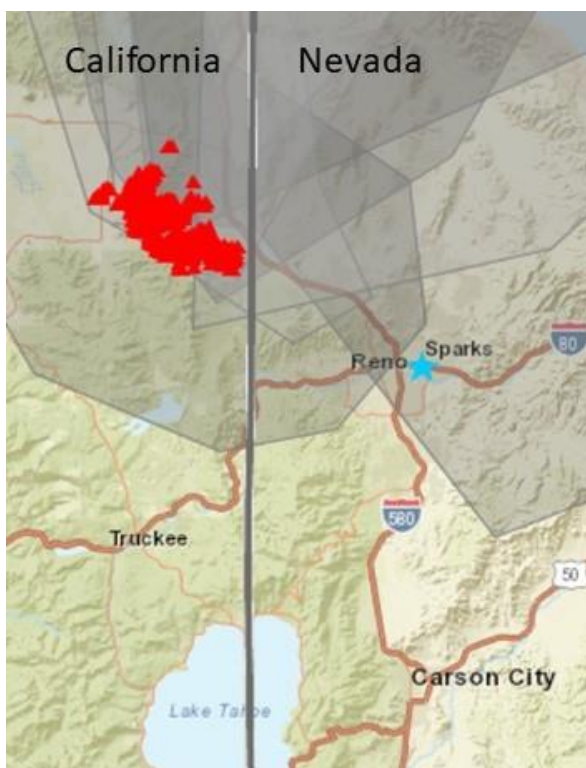
- 255 Satellite monitoring for air quality and health, *Annu. Rev. Biomed. Data Sci.*, 4, 417-447,
<https://doi.org/10.1146/annurev-biodatasci-110920-093120>, 2021
- Huangfu, Y., Yuan, B., Wang, S., Wu, C., He, X., Qi, J., et al.. Revisiting acetonitrile as tracer of biomass burning in anthropogenic-influenced environments. *Geophysical Research Letters*, 48, e2020GL092322.
<https://doi.org/10.1029/2020GL092322>, 2021.
- 260 Jaffe D. Evaluation of Ozone Patterns and Trends in 8 Major Metropolitan Areas in the U.S. Final project report for CRC Project A-124, Coordinating Research Council, Alpharetta, GA, March 2021. Available at: http://crcao.org/wp-content/uploads/2021/04/CRC-Project-A-124-Final-Report_Mar2021.pdf
- Jaffe, D. A., Bertschi, I., Jaegle, L., Novelli, P., Reid, J. S., Tanimoto, H., Vingarzan, R., and Westphal, D. L.: Long-range transport of Siberian biomass burning emissions and impact on surface ozone in western North America, *Geophys. Res. Lett.*, 31, L16106–L16106, <https://doi.org/10.1029/2004GL020093>, 2004.
- 265 Jaffe, D. A., O'Neill, S. M., Larkin, N. K., Holder, A. L., Peterson, D. L., Halofsky, J. E., and Rappold, A. G.: Wildfire and prescribed burning impacts on air quality in the United States, *J. Air Waste Manage. Assoc.*, 70, 583-615, <https://doi.org/10.1080/10962247.2020.1749731>, 2020.
- Kahn, R.: A global perspective on wildfires, *Eos*, 101, <https://doi.org/10.1029/2020EO138260>, 2020.
- 270 Kalashnikov, D. A., Schnell, J. L., Abatzoglou, J. T., Swain, D. L., and Singh, D.: Increasing co-occurrence of fine particulate matter and ground-level ozone extremes in the western United States, *Science Advances*, 8, eabi9386, <https://doi.org/10.1126/sciadv.abi9386>, 2022.
- Kaulfus, A. S., Nair, U., Jaffe, D., Christopher, S. A., and Goodrick, S.: Biomass burning smoke climatology of the United States: implications for particulate matter air quality, *Environ. Sci. Technol.*, 51, 11731-11741, <https://doi.org/10.1021/acs.est.7b03292>, 2017.
- 275 Kiser, D., Elhanan, G., Metcalf, W.J., Schneider B., and Grzymalski J.J. SARS-CoV-2 test positivity rate in Reno, Nevada: association with PM_{2.5} during the 2020 wildfire smoke events in the western United States. *J Expo Sci Environ Epidemiol* 31, 797–803 (2021). <https://doi.org/10.1038/s41370-021-00366-w>.
- 280 Kleinman, L. I., Sedlacek III, A. J., Adachi, K., Buseck, P. R., Collier, S., Dubey, M. K., Hodshire, A. L., Lewis, E., Onasch, T. B., Pierce, J. R., Shilling, J., Springston, S. R., Wang, J., Zhang, Q., Zhou, S., and Yokelson, R. J.: Rapid evolution of aerosol particles and their optical properties downwind of wildfires in the western US, *Atmos. Chem. Phys.*, 20, 13319–13341, <https://doi.org/10.5194/acp-20-13319-2020>, 2020.
- Kotchenruther, R. A.: Source apportionment of PM_{2.5} at multiple Northwest U.S. sites: Assessing regional winter wood smoke impacts from residential wood combustion, *Atmos. Environ.*, 142, 210-219, <https://doi.org/10.1016/j.atmosenv.2016.07.048>, 2016.
- 285 Laing, J. R., Jaffe, D. A., Slavens, A. P., Li, W. T., and Wang, W. X.: Can $\Delta\text{PM}_{2.5}/\Delta\text{CO}$ and $\Delta\text{NO}_y/\Delta\text{CO}$ enhancement ratios be used to characterize the influence of wildfire smoke in urban areas?, *Aerosol Air Qual. Res.*, 17, 2413-2423, <https://doi.org/10.4209/aaqr.2017.02.0069>, 2017.
- Laing, J. R., and Jaffe, D. A.: Wildfires are causing extreme PM concentrations in the western United States, *EM*, July, 2019.
- 290 Lu, X., Zhang, L., Yue, X., Zhang, J. C., Jaffe, D. A., Stohl, A., Zhao, Y. H., and Shao, J. Y.: Wildfire influences on the variability and trend of summer surface ozone in the mountainous western United States, *Atmos. Chem. Phys.*, 16, 14687-14702, <https://doi.org/10.5194/acp-16-14687-2016>, 2016.
- 295 Magzamen, S., Gan, R. W., Liu, J., O'Dell, K., Ford, B., Berg, K., Bol, K., Wilson, A., Fischer, E. V., and Pierce, J. R.: Differential cardiopulmonary health impacts of local and long-range transport of wildfire smoke, *GeoHealth*, 5, e2020GH000330, <https://doi.org/10.1029/2020GH000330>, 2021.
- McClure, C. D., and Jaffe, D. A.: US particulate matter air quality improves except in wildfire-prone areas, *P. Natl. Acad. Sci. USA*, 115, 7901-7906, <https://doi.org/10.1073/pnas.1804353115>, 2018.



- Nault, B. A. et al: Secondary organic aerosols from anthropogenic volatile organic compounds contribute substantially to air pollution mortality, *Atmos. Chem. Phys.*, 21, 11201–11224, <https://doi.org/10.5194/acp-21-11201-2021>, 2021.
- 300 O'Dell, K., Hornbrook, R. S., Permar, W., Levin, E. J. T., Garofalo, L. A., Apel, E. C., Blake, N. J., Jarnot, A., Pothier, M. A., Farmer, D. K., Hu, L., Campos, T., Ford, B., Pierce, J. R., and Fischer, E. V.: Hazardous air pollutants in fresh and aged western US wildfire smoke and implications for long-term exposure, *Environ. Sci. Technol.*, 54, 11838–11847, <https://doi.org/10.1021/acs.est.0c04497>, 2020.
- 305 O'Dell, K., Bilsback, K., Ford, B., Martenies, S. E., Magzamen, S., Fischer, E. V., and Pierce, J. R.: Estimated mortality and morbidity attributable to smoke plumes in the United States: not just a western US problem, *GeoHealth*, 5, e2021GH000457, <https://doi.org/10.1029/2021GH000457>, 2021.
- O'Neill, S. M., Diao, M., Raffuse, S., Al-Hamdan, M., Barik, M., Jia, Y., Reid, S., Zou, Y., Tong, D., West, J. J., Wilkins, J., Marsha, A., Freedman, F., Vargo, J., Larkin, N. K., Alvarado, E., and Loesche, P.: A multi-analysis approach for estimating regional health impacts from the 2017 Northern California wildfires, *J. Air Waste Manage. Assoc.*, 71, 791–814, <https://doi.org/10.1080/10962247.2021.1891994>, 2021.
- 310 Permar, W., Wang, Q., Selimovic, V., Wielgasz, C., Yokelson, R. J., Hornbrook, R. S., Hills, A. J., Apel, E. C., Ku, I.-T., Zhou, Y., Sive, B. C., Sullivan, A. P., Collett Jr, J. L., Campos, T. L., Palm, B. B., Peng, Q., Thornton, J. A., Garofalo, L. A., Farmer, D. K., Kreidenweis, S. M., Levin, E. J. T., DeMott, P. J., Flocke, F., Fischer, E. V., and Hu, L.: Emissions of trace organic gases from western U.S. wildfires based on WE-CAN aircraft measurements, *J. Geophys. Res.-Atmos.*, 126, e2020JD033838, <https://doi.org/10.1029/2020JD033838>, 2021.
- 315 Rogers, H. M., Ditto, J. C., and Gentner, D. R.: Evidence for impacts on surface-level air quality in the northeastern US from long-distance transport of smoke from North American fires during the Long Island Sound Tropospheric Ozone Study (LISTOS) 2018, *Atmos. Chem. Phys.*, 20, 671–682, <https://doi.org/10.5194/acp-20-671-2020>, 2020.
- 320 Rolph, G. D., Draxler, R. R., Stein, A. F., Taylor, A., Ruminski, M. G., Kondragunta, S., Zeng, J., Huang, H. C., Manikin, G., McQueen, J. T., and Davidson, P. M.: Description and verification of the NOAA Smoke Forecasting System: the 2007 fire season, *Weather Forecast.*, 24, 361–378, <https://doi.org/10.1175/2008waf2222165.1>, 2009.
- Selimovic, V., Yokelson, R. J., McMeeking, G. R., and Coefield, S.: In situ measurements of trace gases, PM, and aerosol optical properties during the 2017 NW US wildfire smoke event, *Atmos. Chem. Phys.*, 19, 3905–3926, <https://doi.org/10.5194/acp-19-3905-2019>, 2019.
- 325 Selimovic, V., Yokelson, R. J., McMeeking, G. R., and Coefield, S.: Aerosol mass and optical properties, smoke influence on O₃, and high NO₃ production rates in a western U.S. city impacted by wildfires, *J. Geophys. Res.-Atmos.*, 125, e2020JD032791, <https://doi.org/10.1029/2020JD032791>, 2020.
- 330 Singh, H. B., Cai, C., Kaduwela, A., Weinheimer, A., and Wisthaler, A.: Interactions of fire emissions and urban pollution over California: Ozone formation and air quality simulations, *Atmos. Environ.*, 56, 45–51, <https://doi.org/10.1016/j.atmosenv.2012.03.046>, 2012.
- Sorensen, C., House, J. A., O'Dell, K., Brey, S. J., Ford, B., Pierce, J. R., Fischer, E. V., Lemery, J., and Crooks, J. L.: Associations between wildfire-related PM_{2.5} and intensive care unit admissions in the United States, 2006–2015, *GeoHealth*, 5, e2021GH000385, <https://doi.org/10.1029/2021GH000385>, 2021.
- 335 Teakles, A. D., So, R., Ainslie, B., Nissen, R., Schiller, C., Vingarzan, R., McKendry, I., Macdonald, A. M., Jaffe, D. A., Bertram, A. K., Strawbridge, K. B., Leaitch, W. R., Hanna, S., Toom, D., Baik, J., and Huang, L.: Impacts of the July 2012 Siberian fire plume on air quality in the Pacific Northwest, *Atmos. Chem. Phys.*, 17, 2593–2611, <https://doi.org/10.5194/acp-17-2593-2017>, 2017.
- U.S. Environmental Protection Agency (U.S. EPA). 2017 National Emissions Inventory (NEI) Data. <https://www.epa.gov/air-emissions-inventories/2017-national-emissions-inventory-nei-data> (accessed January 21, 2022).
- 340



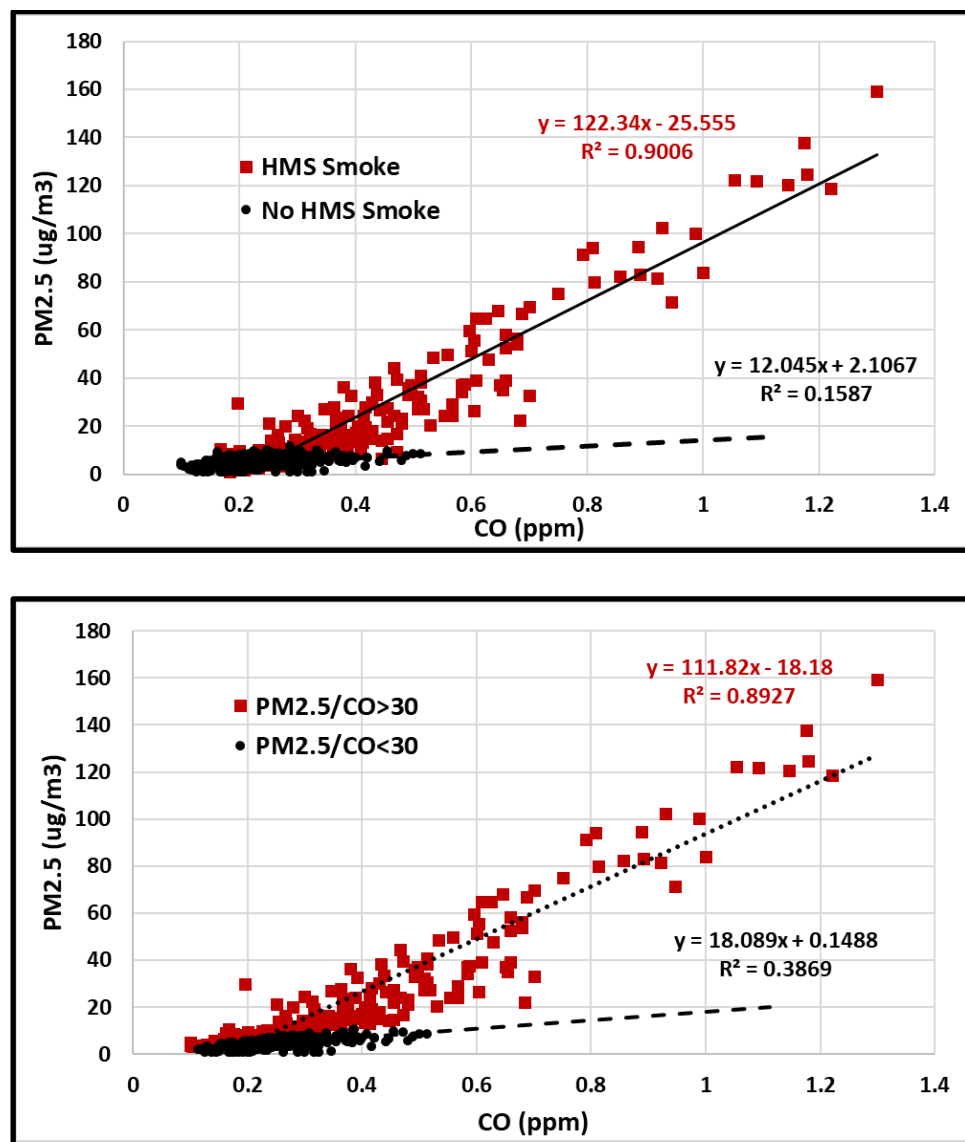
- 345 Ye, X., Arab, P., Ahmadov, R., James, E., Grell, G. A., Pierce, B., Kumar, A., Makar, P., Chen, J., Davignon, D.,
Carmichael, G. R., Ferrada, G., McQueen, J., Huang, J., Kumar, R., Emmons, L., Herron-Thorpe, F. L., Parrington,
M., Engelen, R., Peuch, V. H., da Silva, A., Soja, A., Gargulinski, E., Wiggins, E., Hair, J. W., Fenn, M., Shingler,
T., Kondragunta, S., Lyapustin, A., Wang, Y., Holben, B., Giles, D. M., and Saide, P. E.: Evaluation and
intercomparison of wildfire smoke forecasts from multiple modeling systems for the 2019 Williams Flats fire,
Atmos. Chem. Phys., 21, 14427-14469, <https://doi.org/10.5194/acp-21-14427-2021>, 2021.
- 350 Zhuang, Y., Fu, R., Santer, B. D., Dickinson, R. E., and Hall, A.: Quantifying contributions of natural variability and
anthropogenic forcings on increased fire weather risk over the western United States, P. Natl. Acad. Sci. USA, 118,
e2111875118, <https://doi.org/10.1073/pnas.2111875118>, 2021.



355

Figure 1: NOAA HMS smoke and fire location for Aug. 16, 2020. The Loyaltown fire is burning in California near the Nevada border at this time. The blue star shows the location of the Sparks, NV monitoring site, which is approximately 35-45 km from the fire. This map was created from the AirNowTech site (<https://www.airnowtech.org/>).

360



365 Figure 2: Observed PM_{2.5} vs CO for May-September data (May 1, 2018-August 31, 2021). Each point is the daily mean of observed values sorted by (a) overhead HMS smoke product or (b) PM/CO ratio of 30 μg m⁻³/ppm.

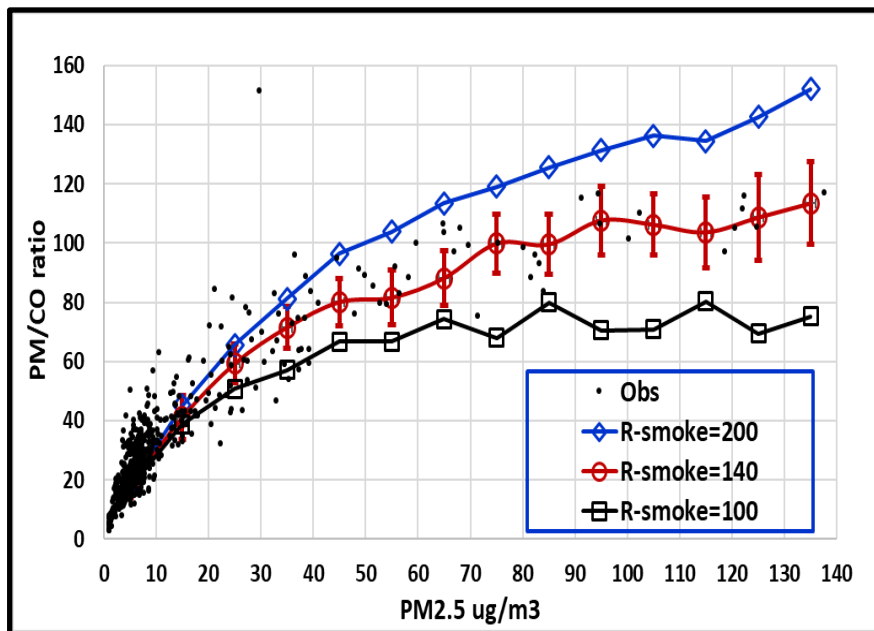


Figure 3. $\text{PM}_{2.5}/\text{CO}$ ratio ($\mu\text{g m}^{-3} \text{ppm}^{-1}$) vs $\text{PM}_{2.5}$. The black dots show the observations, and the black square, red circle and blue diamonds show the influence of the R-smoke parameter for the urban + smoke simulations. The simulation results are binned in $10 \mu\text{g m}^{-3}$ intervals centered on the indicated values. For these simulations, R-urban is fixed at 40. Error bars show 1σ on the middle simulation. One observation is not shown (PM/CO ratio of 122 and a $\text{PM}_{2.5}$ concentration of $159 \mu\text{g m}^{-3}$).

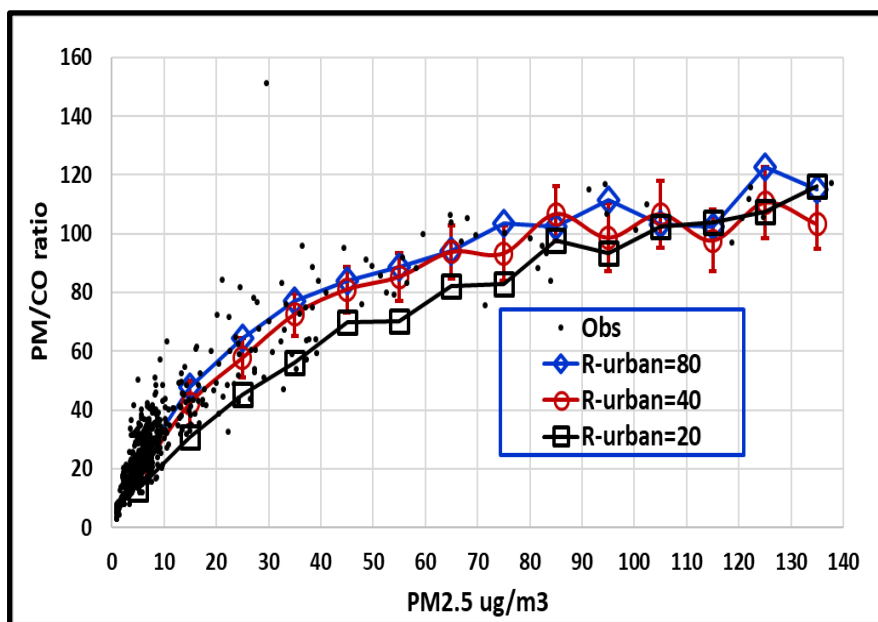
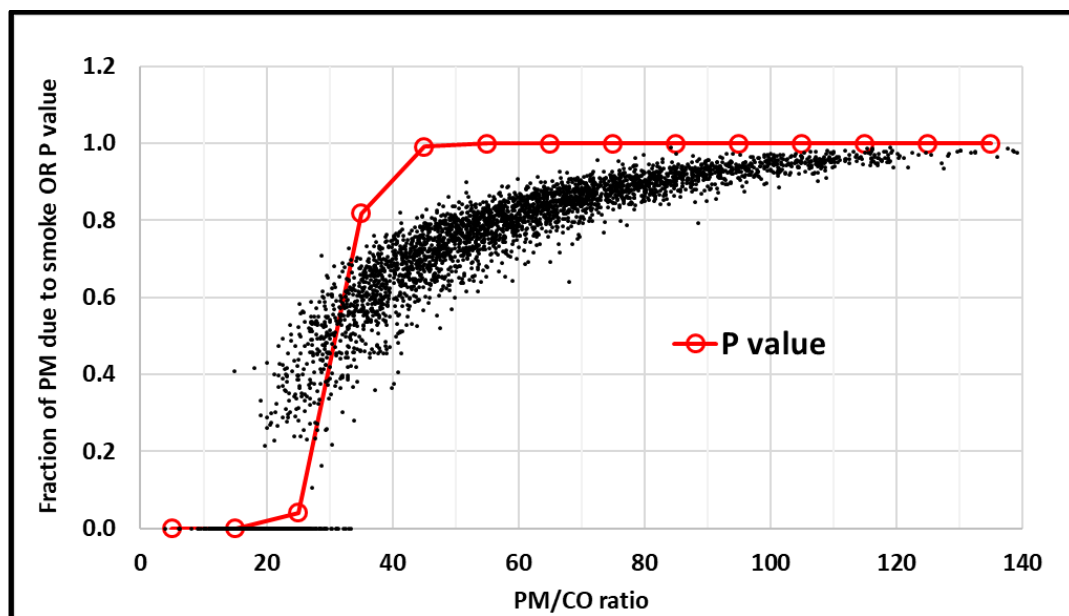


Figure 4. $\text{PM}_{2.5}/\text{CO}$ ratio ($\mu\text{g m}^{-3} \text{ppm}^{-1}$) vs $\text{PM}_{2.5}$. The black dots show the observations, and the black square, red circle and blue diamonds show the influence of the R-urban parameter on the Monte Carlo simulations. The simulation results are binned in $10 \mu\text{g m}^{-3}$ intervals centered on the indicated values. For these simulations, R-smoke is fixed at 140. Error bars show 1σ on the middle simulation. One observation is not shown (PM/CO ratio of 122 and a $\text{PM}_{2.5}$ concentration of $159 \mu\text{g m}^{-3}$).



400



405 **Figure 5.** Fraction of $\text{PM}_{2.5}$ due to smoke vs the $\text{PM}_{2.5}/\text{CO}$ ratio ($\mu\text{g m}^{-3} \text{ppm}^{-1}$) as calculated from the Monte Carlo simulations. We note that the Monte Carlo simulations give a probabilistic relationship. So, for example, at a PM/CO ratio of between 30 and 40, 83% of the points have more than half of the $\text{PM}_{2.5}$ due to smoke. The red open circles show the probability that more than 50% of the $\text{PM}_{2.5}$ is due to smoke, within each PM/CO bin.

410